

Distributed time-varying formation tracking of multi-quadrotor systems with partial aperiodic sampled data

Syed Ali Ajwad, Emmanuel Moulay, Michael Defoort, Tomas Menard, P. Coirault

▶ **To cite this version:**

Syed Ali Ajwad, Emmanuel Moulay, Michael Defoort, Tomas Menard, P. Coirault. Distributed time-varying formation tracking of multi-quadrotor systems with partial aperiodic sampled data. Nonlinear Dynamics, 2022, 108 (3), pp.2263-2278. 10.1007/s11071-022-07294-w . hal-03596635

HAL Id: hal-03596635
https://hal.science/hal-03596635

Submitted on 3 Mar 2022

HAL is a multi-disciplinary open access archive for the deposit and dissemination of scientific research documents, whether they are published or not. The documents may come from teaching and research institutions in France or abroad, or from public or private research centers.

L'archive ouverte pluridisciplinaire **HAL**, est destinée au dépôt et à la diffusion de documents scientifiques de niveau recherche, publiés ou non, émanant des établissements d'enseignement et de recherche français ou étrangers, des laboratoires publics ou privés.

Noname manuscript No.
(will be inserted by the editor)

Distributed time-varying formation tracking of multi-quadrotor systems with partial aperiodic sampled data

Syed Ali Ajwad · Emmanuel Moulay · Michael Defoort · Tomas Ménard · Patrick Coirault

Received: DD Month YEAR / Accepted: DD Month YEAR

Abstract In this article, a distributed formation tracking controller is proposed for Multi-Agent Systems (MAS) consisting of quadrotors. It is considered that each quadrotor in the MAS only shares its translation position information with its neighbors. Moreover, position information is transmitted at nonuniform and asynchronous time instants. The control system is divided into an outer-loop for the position control and an inner-loop for the attitude control. A continuous-discrete time observer is used in the outer-loop to estimate both position and velocity of the the quadrotor and its neighbors using discrete position information it receives. Then, these estimated states are used to design the position controller in order to enable quadrotors to generate the required geometric shape. A finite-time attitude controller is designed to track the desired attitude as dictated by the position controller. Finally, a closed-

S. A. Ajwad
LIAS (EA 6315), Université de Poitiers, 2 rue Pierre Brousse, 86073 Poitiers Cedex 9, France
E-mail: syed.ali.ajwad@univ-poitiers.fr

E. Moulay
XLIM (UMR CNRS 7252), Université de Poitiers, 11 bd Marie et Pierre Curie, 86073 Poitiers Cedex 9, France
E-mail: emmanuel.moulay@univ-poitiers.fr

M. Defoort
LAMIH UMR CNRS 8201, INSA Hauts-de-France, Polytechnic University Hauts-de-France, 59313 Valenciennes, France
E-mail: michael.defoort@uphf.fr

T. Ménard
LAC (EA 7478), Normandie Université, UNICAEN, 6 bd du Maréchal Juin, 14032 Caen Cedex, France
E-mail: tomas.menard@unicaen.fr

P. Coirault
LIAS (EA 6315), Université de Poitiers, 2 rue Pierre Brousse, 86073 Poitiers Cedex 9, France
E-mail: patrick.coirault@univ-poitiers.fr

loop stability analysis of the overall system including nonlinear coupling is performed.

Keywords Multi-agent systems, Quadrotor, Continuous-discrete time observers, Distributed control, Under-actuated system.

1 Introduction

In recent years, the study of Unmanned Air Vehicles (UAV) has attracted much attention due to their vast range of applications in defence, agriculture, transportation, disaster management, entertainment etc. (see for instance [1, 2, 3]). Quadrotor UAV is more popular among other UAVs due to its distinctive characteristics like simple structure, fast maneuverability and vertical take off and landing ability [4]. Compared to a single quadrotor operation, the use of multiple quadrotors working in a cooperative manner has some clear advantages such as high efficiency, flexibility, wide coverage area, robustness, etc.

Formation control or formation tracking of cooperative Multi-Agent System (MAS) is considered as one of the fundamental problems in which agents are required to produce a desired geometric shape in order to accomplish some tasks. Multi-quadrotor formation tracking has various applications both in civilian and military domains. These applications include (but are not limited to) target enclosure and tracking, search and rescue, surveillance, heavy payload transportation and telecommunication relay [5, 6, 7]. The problem of formation control and tracking has been extensively studied in the literature [8, 9, 10, 11, 12]. Formation control techniques are usually categorized as virtual structure [13], behavior-based [14] and leader-follower [15]. Distributed consensus based formation control is another interesting approach in which all above mentioned categories can be incorporated [16]. A consensus-based formation tracking algorithm for second-order MAS has been proposed in [17]. In [18], the formation control problem of MAS with switching topology has been discussed for second-order agent dynamics. A fixed-time formation tracking controller has been proposed for MAS using adaptive neural networks and minimal learning parameter based approach [19]. The problem of formation control for high-order nonlinear systems has been studied in [12, 20].

Nevertheless, it should be noted that the extension of formation tracking algorithms designed for first-order, second-order or even high-order nonlinear MAS to multi-quadrotor systems is not trivial. Indeed, the control design for quadrotors is considered as a complex problem because such systems are not only inherently nonlinear but also under-actuated. The control of multiple quadrotors in a distributed manner becomes even more complex. There exist some works in the literature dealing with the problem of formation control for multi-quadrotors. For instance, a consensus based fixed formation tracking controller has been proposed for multi-quadrotor systems in [21]. In this work, it was considered that the quadrotor flies slowly and propeller respond is very high. The nonlinearity of the system was ignored by linearizing its

vertical model around the equilibrium point and the horizontal movement was described as a fourth-order system. A consensus based formation tracking controller has been designed in [22] where the quadrotor dynamics was divided into two subsystems describing horizontal and vertical motion separately. The formation tracking problem of multi-quadrotor systems in the presence of switching topology has been discussed in [23] using a hierarchical controller for each quadrotor based on position and attitude loops. In [24], a formation tracking algorithm for time-varying formation has been presented. A formation tracking control scheme has been proposed in [25] where the position and attitude dynamics are considered as two subsystems and two controllers are designed separately to control both subsystems. However, the closed-loop stability analysis was not provided.

Another important issue in the above mentioned algorithms is the assumption that both position and velocity states are shared between the neighbours in continuous time. However, in order to reduce the cost and size of the quadrotor, it is of great interest to use a minimum number of sensors. Furthermore, the network may have limited communication resources. It is always more cost effective if the neighbors only share partial data as it requires less communication bandwidth. Therefore, it is not always possible or feasible to transmit the whole state. Similarly, only discrete data can be shared due to digital nature of the communication equipment. Furthermore, transmitting data with uniform and synchronized sampling time is also not possible in many practical applications. To deal with these above mentioned communication constraints, a continuous-discrete time observer based algorithm for consensus (resp. formation tracking) has been proposed [26] (resp. [27, 28]). However, these articles only focus on double-integrator MAS systems. A leader-following consensus algorithm for a fully actuated N-order MAS with Lipschitz nonlinearities is presented in [29]. However, it is not straightforward to extend this technique for the time-varying formation tracking problem of under-actuated nonlinear multi-quadrotor systems.

Inspired by the above discussion, in this paper, a distributed time-varying formation tracking strategy is designed for under-actuated multi-quadrotor systems with communication constraints. It is considered that each quadrotor only shares its translation position information with its neighbors. Velocity and acceleration information is not available. Moreover, the sampling rate at which the position data is transmitted is nonuniform and asynchronous. As mentioned above, irregular and asynchronous sampling is inevitable in all practical applications and exchange of partial state is always cost effective. Therefore, our designed algorithm is useful in all practical applications of multi-quadrotor formation tracking. In the current article, the control system of each quadrotor in the network is divided into a position subsystem (outer-loop) and an attitude subsystem (inner-loop). Both subsystems are coupled with a nonlinear coupling term. First, in the outer-loop, a distributed consensus based position formation tracking algorithm is designed. A continuous-discrete time observer is used to reconstruct both position and velocity in continuous time using the available discrete position data. Then, a finite-time control algorithm is

used in the inner-loop to track the desired attitude. Finally, the stability of the closed-loop system, which includes the nonlinear coupling term, is proved. This kind of cascaded controller architecture for a single quadrotor can be found in the literature [30, 31]. However, the closed-loop stability for multi-quadrotor systems with two coupled control loops has never been carefully analyzed. The stability analysis of multi-quadrotor systems is always more complex when compared to single quadrotor systems especially when multi-quadrotor systems are subjects to communication constraints. The proposed strategy yields first results of outer-inner loop based multi-quadrotor formation control in the presence of communication constraints. The efficiency of the proposed algorithm is shown through simulation results.

The remaining of the paper is organized as follows. Section 2 provides some preliminaries on graph theory while Section 3 describes the system modeling and problem statement. Main results are presented in Section 4 which include controller design and stability analysis. Simulation results are given in Section 5 while the paper is concluded in Section 6.

2 Preliminaries

The communication topology among the agents in a MAS can be described by a graph. Let $\mathcal{G} = (\mathcal{V}, \mathcal{E})$ be a N-order directed graph with $\mathcal{V} = \{v_1, v_2 \dots v_N\}$ denoting a nonempty and finite set of nodes while $\mathcal{E} \subseteq \mathcal{V} \times \mathcal{V}$ represents a set of edges. (v_i, v_j) is an edge of $\mathcal{G}$ which describes that node v_j can receive data from node v_i. In a directed graph, $(v_i, v_j) \in \mathcal{E}$ does not imply that $(v_j, v_i) \in \mathcal{E}$. $\mathcal{A} = [a_{ij}]_{N\times N}$ is the adjacency matrix with $a_{ij} = 1$ if $(v_i, v_j) \in \mathcal{E}$ and $a_{ij} = 0$ otherwise. $\mathcal{L} = [l_{ij}]_{N\times N}$ is the Laplacian matrix given as $l_{ii} = \sum_{j\neq i} a_{ij}$, $l_{ij} = -a_{ij}$ for $i \neq j$. The connectivity between the leader and the N followers is given by a diagonal matrix $\mathcal{B} = \text{diag}(b_1, b_2, \dots, b_N)$ such that $b_i = 1$ if follower i can receive information from the leader and $b_i = 0$ otherwise. A graph has a directed spanning tree if there exists a directed path from the root to all other nodes. See Appendix B of [32] for further details on graph theory.

Assumption 1 *It is assumed that there exists at least one directed spanning tree with the leader as a root, i.e there is at least one directed path from the leader to all the followers.*

Matrix $\mathcal{H} = \mathcal{L} + \mathcal{B}$ is a nonsingular M-matrix due to Assumption 1 [33]. Furthermore, there exists a diagonal matrix $\Omega = \text{diag}(\omega_1, \dots, \omega_N)$ such that $\mathcal{H}^T\Omega + \Omega\mathcal{H} > 0$ [34]. Let

$$\omega_{max} = \max\{\omega_1, \dots, \omega_N\} \tag{1}$$

$$\rho = \lambda_{min}(\mathcal{H}^T\Omega + \Omega\mathcal{H}) \tag{2}$$

where $\lambda_{min}(.)$ represents the corresponding smallest eigenvalue.

3 Problem statement

3.1 System modeling

Let us consider a multi-quadrotor system consisting of N quadrotors. Let the position of the $i-$th quadrotor in the inertial frame $\{I\}$ be represented as $\xi_i = [x_i \ y_i \ z_i]^T$ while the Euler angles are $\eta_i = [\phi_i \ \theta_i \ \psi_i]^T$ where ϕ_i, θ_i and ψ_i represent roll, pitch and yaw angles respectively in the body frame $\{B\}$ as shown in Figure 1.

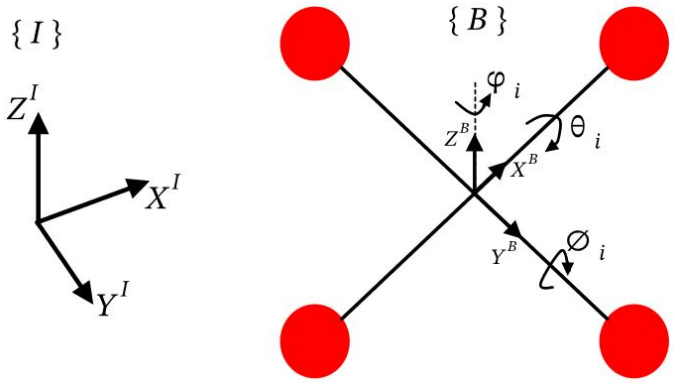


Fig. 1: Inertial and body frames for a quadrotor system.

The quadrotor position dynamics is given as

$$\begin{cases} \ddot{x}_i = \frac{T_i}{m_i}(\cos\phi_i \sin\theta_i \cos\psi_i + \sin\phi_i \sin\psi_i), & i = 1, \ldots, N \\ \ddot{y}_i = \frac{T_i}{m_i}(\cos\phi_i \sin\theta_i \sin\psi_i - \sin\phi_i \cos\psi_i) \\ \ddot{z}_i = \frac{T_i}{m_i}(\cos\phi_i \cos\theta_i) - g \end{cases} \tag{3}$$

where T_i is the total thrust, m_i represents the mass of quadrotor i while g denotes the acceleration due to gravity. The attitude dynamics of quadrotor i can be represented as

$$\begin{cases} \dot{\eta}_i = W_i \Omega_i \\ I_i \dot{\Omega}_i = \Omega_i^* I_i \Omega_i + \tau_i \end{cases} \tag{4}$$

where $\Omega_i = [\omega_{i,1} \ \omega_{i,2} \ \omega_{i,3}]^T$ represents angular velocities in the body frame while Ω_i^* is its skew-symmetric matrix

$$\Omega_i^* = \begin{bmatrix} 0 & -\omega_{i,3} & \omega_{i,2} \\ \omega_{i,3} & 0 & -\omega_{i,1} \\ -\omega_{i,2} & \omega_{i,1} & 0 \end{bmatrix} \tag{5}$$

$I_i = diag\{I_{i,1}, I_{i,2}, I_{i,3}\}$ is the inertia matrix in the body frame, $\tau_i = [\tau_{\phi_i}\ \tau_{\theta_i}\ \tau_{\psi_i}]^T$ represents the torque vector and W_i is the orthogonal rotation matrix given as

$$W_i = \begin{bmatrix} 1 & \sin\phi_i \tan\theta_i & \cos\phi_i \tan\theta_i \\ 0 & \cos\phi_i & -\sin\phi \\ 0 & \frac{\sin\phi_i}{\cos\theta_i} & \frac{\cos\phi_i}{\cos\theta_i} \end{bmatrix} \tag{6}$$

The quadrotors dynamics (3) and (4) can be written in a more compact form as

$$\begin{cases} \ddot{\xi}_i = \frac{T_i}{m_i}\mathcal{R}_{\mathcal{B}}^{\mathcal{I}} e_3 - g e_3, \qquad i = 1, \ldots, N \\ \ddot{\eta}_i = \dot{W}_i \Omega_i + W_i I_i^{-1} \Omega_i^* I_i \Omega_i + W_i I_i^{-1} \tau_i \end{cases} \tag{7}$$

where $e_3 = [0, 0, 1]^T$ while $\mathcal{R}_{\mathcal{B}}^{\mathcal{I}} \in SO(3)$ denotes the rotation matrix between the body frame and the inertial frame

$$\mathcal{R}_{\mathcal{B}}^{\mathcal{I}} = \begin{bmatrix} c\theta_i c\psi_i & s\phi_i s\theta_i c\psi_i - c\phi_i s\psi_i & c\phi_i s\theta_i c\psi_i + s\phi_i s\psi_i \\ c\theta_i s\psi_i & s\phi_i s\theta_i c\psi_i + c\phi_i s\psi_i & c\phi_i s\theta_i c\psi_i - s\phi_i s\psi_i \\ -s\theta_i & s\phi_i c\theta_i & c\phi_i c\theta_i \end{bmatrix} \tag{8}$$

where c and s represent cos(.) and sin(.), respectively.

The overall quadrotor system is under-actuated since there are four control inputs $(T_i, \tau_{\phi_i}, \tau_{\theta_i}, \tau_{\psi_i})$ and six outputs $(x_i, y_i, z_i, \phi_i, \theta_i, \psi_i)$. Therefore, it is not possible to control all the outputs directly. However, if only the attitude dynamics is considered, it is clear that it is fully actuated. Hence, (7) can be written as

$$\begin{cases} \ddot{\xi}_i = \frac{T_i}{m_i}\mathcal{R}_{\mathcal{B}}^{\mathcal{I}} e_3 - g e_3 \\ \ddot{\eta}_i = \tilde{\tau}_i \end{cases} \tag{9}$$

with $\tilde{\tau}_i = \dot{W}_i \Omega_i + W_i I_i^{-1} \Omega_i^* I_i \Omega_i + W_i I_i^{-1} \tau_i$.

3.2 Problem formulation

The desired formation pattern can be defined by a formation vector $F(t) = [f_1(t)^T \ldots f_N(t)^T]$ where $f_i(t) = [f_{i,\xi}^T, f_{i,v}^T]$ satisfies

$$\dot{f}_{i,\xi} = f_{i,v}$$

for $i = 1, \ldots, N$. $f_{i,\xi},\ f_{i,v} \in \mathbb{R}^3$ are the corresponding position and velocity offsets of quadrotor i with respect to the reference trajectory $r_0 = [\xi_0\ \dot{\xi}_0]^T$ where $\xi_0 = [x_0\ y_0\ z_0]$. The reference trajectory can be independently produced by a real or virtual leader denoted with 0. It is worth noting that the formation vector f_i only describes the offset with respect to the leader and does not represent formation coordinates in the global frame. To further explain the

notation of formation vector $f_i(t)$, let us consider a network of quadrotors with a leader and three followers. Let the formation vector be chosen as

$$f_i(t) = \begin{pmatrix} 10\cos(0.1t + 2\pi(i-1)/3) \\ 10\sin(0.1t + 2\pi(i-1)/3) \\ 3(i-1) - 3 \\ -\sin(0.1t + 2\pi(i-1)/3) \\ \cos(0.1t + 2\pi(i-1)/3) \\ 0 \end{pmatrix} \tag{10}$$

for $i = 1, 2, 3$. This formation vector defines that the followers move around the leader in a circle of radius 10m with a phase difference of $2\pi/3$. The altitude position offsets are constant with values -3m, 0m and 3m for follower 1, 2 and 3 respectively. A visual illustration of this formation is provided in Figure 2.

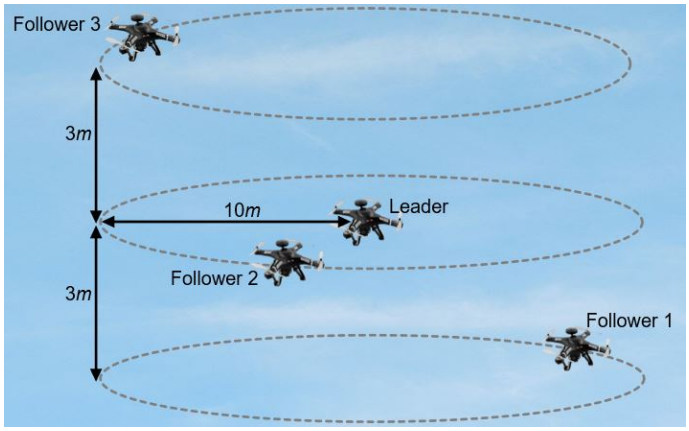


Fig. 2: Example of time-varying formation.

Definition 1 The formation tracking problem of a multi-quadrotor system is said to be practically solved if there exists $\bar{\epsilon} \geq 0$ such that

$$\limsup_{t \to +\infty} \|r_i(t) - f_i - r_0(t)\| \leq \bar{\epsilon}, \qquad i = 1, \ldots, N$$

where $r_i = [\xi_i \ \dot{\xi}_i]^T$ for $i = 1, \ldots, N$.

The objective of quadrotors is to achieve time-varying formation in the 3D plane. It is considered that each quadrotor in the network sends only its position state to its neighbors at nonuniform and asynchronous sampling times. Only a few quadrotors in the network have access to the discrete reference position. Let $t_k^{i,j}$ be the instant when quadrotor j transmits its position information to quadrotor i where $i = 1, \ldots, N$, $j = 0, \ldots, N$ $(j \neq i)$ and $k \in \mathbb{N}$ such that

$$0 < t_{k+1}^{i,j} - t_k^{i,j} < \tau_M$$

where τ_M is the maximum allowable sampling time.

4 Distributed time-varying formation tracking controller

Let us set $\xi_{di} = f_{i,\xi} + \xi_0$. Then, the tracking error vector can be defined as

$$e_{\xi_i} = [\xi_i - \xi_{di}, \dot{\xi}_i - \dot{\xi}_{di}]^T \tag{11}$$

Now let $\eta_{di} = [\phi_{di}\ \theta_{di}\ \psi_{di}]^T$ be the desired attitude. The attitude error vector can be given as

$$e_{\eta_i} = [\eta_i - \eta_{di}\ \dot{\eta}_i - \dot{\eta}_{di}]^T \tag{12}$$

Therefore, one can obtain the following expressions

$$\begin{cases} \dot{e}_{\xi_i} = Ae_{\xi_i} + B(\ddot{\xi}_i - \ddot{\xi}_{di}) \\ \dot{e}_{\eta_i} = Ae_{\eta_i} + B(\ddot{\eta}_i - \ddot{\eta}_{di}) \end{cases} \tag{13}$$

with $A = \begin{pmatrix} 0_3 & I_3 \\ 0_3 & 0_3 \end{pmatrix}$, $B = \begin{pmatrix} 0_3 \\ I_3 \end{pmatrix}$. Dynamics (9) can be seen as a cascaded structure where position and attitude subsystems are coupled through the rotation matrix $\mathcal{R}_{\mathcal{B}}^{\mathcal{I}}$. Indeed, let us define the virtual control $\mu_i = [\mu_{xi}\ \mu_{yi}\ \mu_{zi}]^T$ as in [30]

$$\begin{cases} \mu_{x_i} = \frac{T_i}{m_i}(c\phi_{di}s\theta_{di}c\psi_{di} + s\phi_{di}s\psi_{di}) \\ \mu_{y_i} = \frac{T_i}{m_i}(c\phi_{di}s\theta_{di}s\psi_{di} - s\phi_{di}s\psi_{di}) \\ \mu_{z_i} = \frac{T_i}{m_i}(c\phi_{di}c\theta_{di}) - g \end{cases} \tag{14}$$

The thrust and desired angles can be obtained as

$$T_i = m_i\sqrt{\mu_{x_i}^2 + \mu_{y_i}^2 + (\mu_{z_i} + g)^2} \tag{15}$$

$$\phi_{di} = \sin^{-1}\left(\frac{m_i}{T_i}(\mu_{x_i}\sin\psi_{di} - \mu_{y_i}\cos\psi_{di})\right) \tag{16}$$

$$\theta_{di} = \tan^{-1}\left(\frac{\mu_{x_i}\cos\psi_{di} + \mu_{y_i}\sin\psi_{di}}{\mu_{z_i} + g}\right) \tag{17}$$

while the desired yaw angle ψ_{di} is independant of other states. Now introducing μ_i and replacing (9) in (13), one can get

$$\begin{cases} \dot{e}_{\xi_i} = \underbrace{Ae_{\xi_i} + B\left(\mu_i - \ddot{\xi}_{di}\right)}_{f_{\xi_i}} + \underbrace{\frac{T_i}{m_i}BH_i(\eta_i, \eta_{di})}_{f_{\Delta i}} \\ \dot{e}_{\eta_i} = \underbrace{Ae_{\eta_i} + B\left(\tilde{\tau}_i - \ddot{\eta}_{di}\right)}_{f_{\eta_i}} \end{cases} \tag{18}$$

where $H_i(\eta_i, \eta_{di}) = [h_1\ h_2\ h_3]^T$ and

$$\begin{cases} h_1 = c\phi_i s\theta_i c\psi_i + s\phi_i s\psi_i - (c\phi_{di}s\theta_{di}c\psi_{di} + s\phi_{di}s\psi_{di}) \\ h_2 = c\phi_i s\theta_i c\psi_i - s\phi_i s\psi_i - (c\phi_{di}s\theta_{di}c\psi_{di} - s\phi_{di}s\psi_{di}) \\ h_3 = c\phi_i c\theta_i - c\phi_{di}c\theta_{di} \end{cases} \tag{19}$$

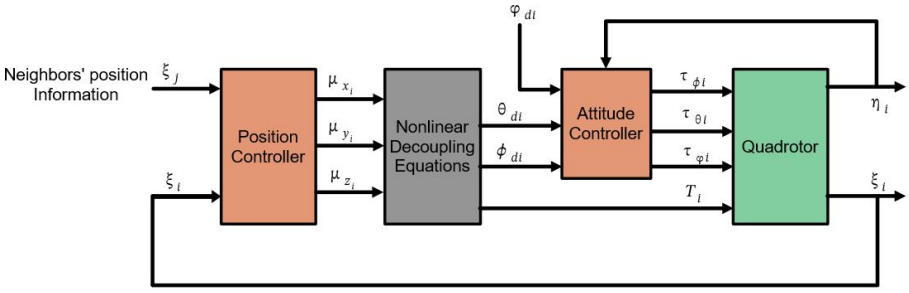


Fig. 3: Overall control architecture of quadrotor i

System (18) can be seen as two linear subsystems coupled by a nonlinear term $f_{\Delta i}$. The control objective then becomes to design μ_i and $\tilde{\tau}_i$ such that the position and attitude errors converge asymptotically.

The overall control design of quadrotor i can be obtained in the following steps:

1. Design a distributed control scheme μ_i for the subsystem $\dot{e}_{\xi_i} = f_{\xi_i}$ while first ignoring the coupling term $f_{\Delta i}$;
2. Design a control law $\tilde{\tau}$ for the subsystem $\dot{e}_{\eta_i} = f_{\eta_i}$ such that the tracking error e_{η_i} converges to zero asymptotically;
3. Finally, consider the closed-loop system including the coupling term $f_{\Delta i}$ and show that e_{ξ_i} and e_{η_i} still converge to zero.

Figure 3 shows the control architecture of the i^{th} quadrotor in the network.

4.1 Controller Design

4.1.1 Position controller design

Let us first consider the position subsystem. It can be seen that the subsystem $\dot{e}_{\xi_i} = f_{\xi_i}$ corresponds to the following dynamics

$$\ddot{\xi}_i = \mu_i \tag{20}$$

It is considered that each quadrotor can measure and transmit its position state ξ_i only. The velocity $\dot{\xi}_i$ and the acceleration $\ddot{\xi}_i$ are not available. The position ξ_i is transmitted only at irregular and nonuniform time instants. The state-space representation of (20) can be given as

$$\begin{cases} \dot{r}_i = Ar_i + B\mu_i \\ y_i = Cr_i \end{cases} \tag{21}$$

with $C = [I_3\ 0_3]$. Let us consider that the reference trajectory is produced by a virtual leader with the same dynamics, i.e.,

$$\begin{cases} \dot{r}_0 = Ar_0 + B\mu_0 \\ y_0 = Cr_0 \end{cases} \tag{22}$$

The input of the leader, i.e. μ_0, is not affected by other quadrotors in the network. It can be designed to achieve any required reference trajectory for the following quadrotors. Only the following assumption is made.

Assumption 2 *The input of the leader $\mu_0(t)$ is bounded by a constant $\delta_0 \geq 0$, i.e. one has $\|\mu_0(t)\| \leq \delta_0$ for all $t \geq 0$.*

The control input for formation tracking is given by

$$\begin{aligned}\mu_i(t) =& \dot{f}_{i,v} - \bar{c}K_1^2 \left[\sum_{j=1}^{N} a_{ij}\left(\hat{\xi}_{i,i}(t) - f_{i,\xi} - \hat{\xi}_{i,j}(t) + f_{j,\xi}\right)\right. \\ &\left. + b_i\left(\hat{\xi}_{i,i}(t) - f_{i,\xi} - \hat{\xi}_{i,0}(t)\right)\right] \\ &- \bar{2}cK_1 \left[\sum_{j=1}^{N} a_{ij}\left(\hat{v}_{i,i}(t) - f_{i,v} - \hat{v}_{i,j}(t) + f_{j,v}\right)\right. \\ &\left. + b_i\left(\hat{v}_{i,i}(t) - f_{i,v} - \hat{v}_{i,0}(t)\right)\right] \end{aligned} \tag{23}$$

where K_1 and $\bar{c}$ denote the controller gain and coupling strength respectively while $\hat{\xi}_{i,j} \in \mathbb{R}^3$ and $\hat{v}_{i,j} \in \mathbb{R}^3$ are the estimated position and velocity of quadrotor j by quadrotor i and are given by

$$\dot{\hat{r}}_{i,j}(t) = A\hat{r}_{i,j}(t) - K_2\Delta^{-1}K_o e^{-2K_2(t-\kappa_{i,j}(t))}\left(\hat{\xi}_{i,j}(\kappa_{i,j}(t)) - \xi_j(\kappa_{i,j}(t))\right) \tag{24}$$

with $\hat{r}_{i,j}(t) = \left[\hat{\xi}_{i,j}^T\ \hat{v}_{i,j}^T\right]^T$, $\Delta = \begin{pmatrix} I_m & 0_m \\ 0_m & \frac{1}{K_2}I_m \end{pmatrix}$, $K_o = \left[2I_m\ I_m\right]^T$ while K_2 represents the observer tuning parameter. $\kappa_{i,j}(t) = \max\left\{t_k^{i,j} \mid t_k^{i,j} \leq t, k \in \mathbb{N}\right\}$ is the last instant when quadrotor i receives the position data of quadrotor j. The above expression (24) represents a high-gain continuous-discrete time observer which estimates position and velocity of a quadrotor as well as its neighbors in continuous time from discrete position data.

Remark 1 Here, the coupling strength $\bar{c}$ is chosen beforehand and remains constant for all $t \geq 0$ since only fixed topology is considered. Therefore, for all $t \geq 0$, quadrotors only use local information to achieve the required formation pattern. The requirement of knowing the communication topology for the controller parameters is a common practice in cooperative control. In future work, one may investigate the use of adaptive gains to avoid such assumption.

4.1.2 Attitude controller design

First, the following notations are introduced. For any non-negative real number α and for any $x \in \mathbb{R}$,

$$sig^{\alpha}(x) = sign(x)|x|^{\alpha} \tag{25}$$

$$fsig^{\alpha}(x) = \begin{cases} x, & |x| > 1 \\ sig^{\alpha}(x), & |x| \leq 1 \end{cases} \tag{26}$$

Let us now consider the attitude subsystem

$$\dot{e}_{\eta_i} = f_{\eta_i} = Ae_{\eta_i} + B\left(\tilde{\tau}_i - \ddot{\eta}_{di}\right) \tag{27}$$

with the following attitude input

$$\tilde{\tau}_i = \ddot{\eta}_{di} - K_3 fsig^{\alpha_3}(\eta_i - \eta_{di}) - K_4 fsig^{\alpha_4}(\dot{\eta}_i - \dot{\eta}_{di}) \tag{28}$$

where $K_3, K_4 > 0$.

Lemma 1 *[25] For the attitude error dynamics* (27) *with control law* (28)*, the desired attitude is achieved in finite time, i.e.* $\|\eta_i - \eta_{di}\| \to 0$ *if* α_3 *and* α_4 *are chosen as* $0 < \alpha_3 < 1$ *and* $\alpha_4 = 2\alpha_3/(1 + \alpha_3)$*.*

4.2 Closed-loop stability analysis

The following is an important lemma for stability analysis of cascade systems.

Lemma 2 *Let* $v_1(t)$ *and* $v_2(t)$ *be real valued functions verifying*

$$\begin{aligned} \frac{d}{dt}\left(v_1^2(t) + v_2^2(t)\right) \leq -av_1^2(t) - bv_2^2(t) + c\int_{t-\delta}^{t} v_2^2(s)ds \\ +g(t)(v_1^2(t) + v_2^2(t)) + k, \end{aligned} \tag{29}$$

for all $t \geq 0$*,* $a, b, c, \delta > 0$*,* $k \geq 0$ *and* $g(t)$ *is a decaying function such that for some* $t^* \geq 0$ $g(t) \geq 0$ *if* $0 \leq t \leq t^*$ *and* $g(t) = 0$ *if* $t > t^*$ *. There exist* $\gamma \geq 1$*,* $\varrho > 0$*, independent of* a, b, c, k*, and* $\bar{\alpha} \geq 0$ *such that if* $\delta < \varrho \min\left(\frac{b}{c}, \frac{1}{\sigma}\right)$*, then* $v_1(t)$ *and* $v_2(t)$ *verify the following inequality*

$$v_1^2(t) + v_2^2(t) \leq \bar{\alpha}e^{-\sigma t} + \frac{\gamma k}{\sigma}, \quad \forall t \geq 0 \tag{30}$$

where σ *is given by*

$$\sigma = \frac{1}{2}\min(a, b) \tag{31}$$

The proof of Lemma 2 is provided in Appendix A.

Remark 2 It is worth mentioning that Lemma 2 is more general than Lemma 2 from [29] due to the presence of term $g(t)(v_1^2(t)+v_2^2(t))$ in (29). Such term should be here considered due to the coupling between position subsystem (outer-loop) and attitude subsystem (inner-loop), making the stability analysis of the closed-loop system in the current paper different from [29].

Theorem 1 *Given the position controller* (23) *and the attitude controller* (28)*, if Assumptions 1-2 hold and if the control parameters satisfy*

$$K_2 \leq \frac{\bar{\varrho}}{\tau_M} \tag{32}$$

$$\bar{c} \geq \frac{\omega_{max}}{\rho} \tag{33}$$

$$K_1 = \epsilon K_2 \tag{34}$$

with $\epsilon \in (0,1)$ *and* $\bar{\varrho} > 0$*, then the formation tracking of the multi-quadrotor system* (9) *is achieved in the sense of Definition 1.*

Proof It is clear from Lemma 1 that the attitude error dynamics $\dot{e}_{\eta_i} = Ae_{\eta_i} + B\left(\tilde{\tau}_i - \ddot{\eta}_{di}\right)$ (given in (18)) using attitude control input (28), converges to zero in finite time. Now, it is needed to show that the position error dynamics including the coupling term also converges. It is worth mentioning that this coupling makes the stability analysis of the closed-loop system in the current paper different from [29].

The remaining of the proof is divided into several steps. In the first step, the dynamics of the position and estimation errors are derived and written in a compact form along with the time-varying formation controller (23). Appropriate coordinate transformation is also introduced in step 1. Position and observer errors are combined in new variables in step 2 to get a more compact form. In step 3, candidate Lyapunov functions are introduced and inequalities involving their derivatives are derived. Lemma 2 is applied in step 4 to show the convergence of the formation tracking error with formation controller (23) and (28).

Step 1. Consider the position error dynamics with the coupling term from (18)

$$\dot{e}_{\xi_i} = \underbrace{Ae_{\xi_i} + B\mu_i - B\mu_0}_{f_{\xi_i}} + \underbrace{\frac{T_i}{m_i} BH_i(\eta_i, \eta_{di})}_{f_{\Delta i}} \tag{35}$$

Define the estimation error as $\tilde{x}_{i,j} = \hat{r}_{i,j} - r_i$ for $i = 1, \ldots N$ and $j = 0, \ldots N$, one has

$$\dot{\tilde{x}}_{i,j}(t) = (A - \theta\Delta^{-1}K_oC)\tilde{x}_{i,j}(t) - \theta\Delta^{-1}K_o z_{i,j}(t) - B\mu_j(t)$$

where $z_{i,j}(t) = \left[e^{-2\theta(t-\kappa_{i,j}(t))}C\tilde{x}_{i,j}(\kappa_{i,j}(t)) - C\tilde{x}_{i,j}(t)\right]$.

The position control input can be written as

$$\mu_i = -\bar{c}K_c\Gamma\sum_{k=1}^{N}\mathcal{H}_{ik}e_{\xi_k} - \bar{c}K_c\Gamma\sum_{k=1}^{N}\mathcal{H}_{ik}\tilde{x}_{i,k} + b_i\bar{c}K_c\Gamma\tilde{x}_{i,0}$$

for $i = 1, \ldots, N$ and $K_c = B^T Q = \begin{pmatrix} I_3 & 2I_3 \end{pmatrix}$ with Q the symmetric positive definite matrix solution of $Q + QA + A^T Q = QBB^T Q$ and $\Gamma = \begin{pmatrix} K_1^2 I_3 & 0_3 \\ 0_3 & K_1 I_3 \end{pmatrix}$

Applying the coordinate transformation for high-gain design as $\bar{e}_{\xi_i} = \Gamma e_{\xi_i}$ and $\bar{x}_{i,j} = \Delta \tilde{x}_{i,j}$, one has

$$\dot{\bar{e}}_{\xi_i}(t) = K_1 A \bar{e}_{\xi_i}(t) + K_1 B \mu_i(t) - K_1 B \mu_0(t) + \frac{K_1 T_i}{m_i} B H_i$$

$$\dot{\bar{x}}_{i,j}(t) = K_2(A - K_o C)\bar{x}_{i,j}(t) - K_2 K_o z_{i,j}(t) - \frac{1}{K_2} B \mu_j(t)$$

$$\mu_i = -\bar{c} K_c \sum_{k=1}^{N} \mathcal{H}_{ik} \bar{e}_{\xi_k} - \bar{c} K_c \Gamma \Delta^{-1} \sum_{k=1}^{N} \mathcal{H}_{ik} \bar{x}_{i,k} + b_i \bar{c} K_c \Gamma \Delta^{-1} \bar{x}_{i,0}$$

Step 2. Let $e_\xi^c = [\bar{e}_{\xi_1}^T \ldots \bar{e}_{\xi_N}^T]^T$, $\bar{x}_i^o = [(\bar{x}_{i,1})^T \ldots (\bar{x}_{i,N})^T]^T$, $i = 1 \ldots N$ and $\bar{x}_0^o = [(\bar{x}_{1,0})^T \ldots (\bar{x}_{N,0})^T]$. The tracking error dynamics can be written in a more compact form as

$$\dot{e}_\xi^c = K_1[I_N \otimes A]e_\xi^c - \bar{c}K_1[\mathcal{H} \otimes (BK_c)]e_\xi^c - \bar{c}K_1 \sum_{i=1}^{N}[(\mathcal{D}_i^N \mathcal{H}) \otimes (BK_c\Gamma\Delta^{-1})]\bar{x}_i^o$$
$$+\bar{c}K_1[I_N \otimes (BK_c\Gamma\Delta^{-1})][\mathcal{B} \otimes I_6]\bar{x}_0^o - K_1[\mathbf{1}_N \otimes B]\mu_0 + K_1[I_N \otimes B]F_\Delta$$

where $F_\Delta = [\frac{T_1}{m_1} H_1, \ldots, \frac{T_N}{m_N} H_N]^T$.

Step 3. Now, let us define the following Lyapunov functions

$$\bar{V}_c(e_\xi) = e_\xi^T [\Omega \otimes Q] e_\xi \tag{36}$$

$$V_o(\bar{x}_{i,j}) = (\bar{x}_{i,j})^T P (\bar{x}_{i,j}) \tag{37}$$

$$\bar{V}_o(\bar{x}^o) = \sum_{i=1}^{N} \sum_{j=0}^{N} s_{ij} V_o(\bar{x}_{i,j}) \tag{38}$$

$s_{ij} = 1$ if quadrotor i receives information from quadrotor j and 0 otherwise for $i = 1, \ldots, N$, $j = 0, \ldots, N$ and $\bar{x}^o$ is the vector containing all the $\bar{x}_{i,j}$ such that $s_{ij} = 1$.

The derivative of $V(e_\xi)$ can be computed as

$$\begin{aligned}
\dot{\bar{V}}_c(e_\xi^c) = {} & K_1(e_\xi^c)^T[\Omega \otimes (A^T Q + QA)]e_\xi^c - \bar{c}K_1(e_\xi^c)^T[(\mathcal{H}^T\Omega) \otimes ((BK_c)^T Q)]e_\xi^c \\
& -\bar{c}K_1(e_\xi^c)^T[(\Omega\mathcal{H}) \otimes (QBK_c)]e_\xi^c + 2\bar{c}K_1(e_\xi^c)^T[\Omega \otimes (QBK_c\Gamma\Delta^{-1})][\mathcal{B} \otimes I_{2m}]\bar{x}_0^o \\
& -2\bar{c}K_1 \sum_{i=1}^{N}(e_\xi^c)^T[(\Omega\mathcal{D}_i^N\mathcal{H}) \otimes (QBK^c\Gamma\Delta^{-1})]\bar{x}_i^o \\
& -2K_1(e_\xi^c)^T[(\Omega\mathbf{1}_N) \otimes (QB)]\mu_0 + 2K_1(e_\xi^c)^T[(\Omega \otimes (QB)]F_\Delta
\end{aligned}$$

One can show that

$$\begin{aligned}
& 2K_1(e_\xi^c)^T[(\Omega \otimes (QB)]F_\Delta \\
& \leq 2K_1\bar{k}_3\sqrt{V_c}\sum_{i=1}^{N}\chi\|e_{\eta_i}\|\left[\sqrt{V_c(e_\xi^c)} + \sum_{k=0}^{N} s_{i,k}\sqrt{V_o(\bar{x}_{i,k})}\right]
\end{aligned} \tag{39}$$

where $\bar{k}_3 = \sqrt{\omega_{\max}\lambda_{\max}(Q)}$. The derivation of (39) is given in Appendix B.

Similarly, one has

$$\begin{aligned}
&2\bar{c}K_1(e_\xi^c)^T[\Omega \otimes (QBK_c\Gamma\Delta^{-1})][\mathcal{B} \otimes I_{2m}]\bar{x}_0^o \\
&-2\bar{c}K_1\sum_{i=1}^{N}(e_\xi^c)^T[(\Omega\mathcal{D}_i^N\mathcal{H}) \otimes (QBK_c\Gamma\Delta^{-1})]\bar{x}_i^o \\
&\leq 2k_1K_1\|\Gamma\Delta^{-1}\|\sqrt{\bar{V}_c(e_\xi)}\sqrt{\bar{V}_o(\bar{x}^o)} \qquad (40)\\
&-2K_1(e_\xi)^T[(\Omega\mathbf{1}_N) \otimes (QB)]\mu_0 \leq 2K_1\bar{k}_2\delta_0\sqrt{V_c(e_\xi^c)}. \qquad (41)
\end{aligned}$$

with $k_1, \bar{k}_2 \geq 0$ where k_1 and k_2 are independent of the tuning parameters. and if $\bar{c} \geq \omega_{\max}/\rho$, then one has

$$\begin{aligned}
&K_1(e_\xi)^T[\Omega \otimes (AQ^T + QA)]e_\xi - \bar{c}K_1(e_{\xi_i})^T[(\mathcal{H}^T\Omega) \otimes ((BK_c)^TQ)]e_\xi \\
&-\bar{c}K_1(e_{\xi_i})^T[(\Omega\mathcal{H}) \otimes (QBK_c)]e_\xi \leq -K_1\bar{V}_c(e_\xi) \qquad (42)
\end{aligned}$$

These inequalities lead to

$$\begin{aligned}
\dot{\bar{V}}_c(e_\xi^c) \leq\ & -K_1\bar{V}_c(e_\xi^c) + 2k_1K_1\|\Gamma\Delta^{-1}\|\sqrt{\bar{V}_c(e_\xi)}\sqrt{\bar{V}_o(\bar{x}^o)} + 2\bar{k}_2K_1\delta_0\sqrt{\bar{V}_c(e_\xi)} \\
&+2\bar{k}_3K_1\sqrt{\bar{V}_c(e_\xi^c)}\sum_{i=1}^{N}\chi\|e_{\eta_i}\|\left[\sqrt{V_c(e_\xi)} + \sum_{k=0}^{N}s_{i,k}\sqrt{V_o(\bar{x}_{i,k})}\right]
\end{aligned}$$

Similarly,

$$\begin{aligned}
\dot{\bar{V}}_o(\bar{x}^o) \leq\ & -K_2\bar{V}_o(\bar{x}^o) + 2K_2^2k_4\sqrt{\bar{V}_o(\bar{x}^o)}\int_{t-\tau_M}^{t}\sqrt{\bar{V}_o(\bar{x}^o(s))}ds \\
&+2K_1k_6\bar{V}_o(\bar{x}^o) + 2\frac{k_5}{K_2}\sqrt{\bar{V}_o(\bar{x}^o)}\sqrt{\bar{V}_c(e_\xi)} + 2\frac{k_7}{K_2}\delta_0\sqrt{\bar{V}_o(\bar{x}^o)} \qquad (43)
\end{aligned}$$

with $k_4, k_5, k_6, k_7 \geq 0$ are independent of the tuning parameters.

Step 4. One has

$$\begin{aligned}
&\frac{d}{dt}\left(\sqrt{\bar{V}_c(e_\xi^c)} + \epsilon^{\frac{3}{2}} K_2^2 \sqrt{\bar{V}_o(\bar{x}^o)}\right) \\
&\leq -\frac{\epsilon K_2}{4}\left(1 - 4k_5\epsilon^{\frac{1}{2}}\right)\sqrt{\bar{V}_c(e_\xi^c)} - \frac{\epsilon^{\frac{3}{2}} K_2^3}{4}\left(1 - 4k_1\epsilon^{\frac{1}{2}} - 4k_6\epsilon\right)\sqrt{\bar{V}_o(\bar{x}^o)} \\
&\quad -\frac{\epsilon K_2}{4}\sqrt{\bar{V}_c(e_\xi^c)} - \frac{\epsilon^{\frac{3}{2}} K_2^3}{4}\sqrt{\bar{V}_o(\bar{x}^o)} + k_4\epsilon^{\frac{3}{2}} K_2^4 \int_{t-\tau_M}^{t} \sqrt{\bar{V}_o(\bar{x}^o(s))} ds \\
&\quad +\bar{k}_3\epsilon K_2 \sum_{i=1}^{N} \chi\|e_{\eta_i}\| \left[\sqrt{V_c(e_\xi)} + \sum_{k=0}^{N} s_{i,k}\sqrt{V_o(\bar{x}_{i,k})}\right] + \bar{k}_2\epsilon K_2\delta_0 + k_7\epsilon^{\frac{3}{2}} K_2\delta_0 \\
&\leq -\frac{\epsilon K_2}{4}\left(1 - 4k_5\epsilon^{\frac{1}{2}}\right)\sqrt{\bar{V}_c(e_\xi^c)} - \frac{\epsilon^{\frac{3}{2}} K_2^3}{4}\left(1 - 4k_1\epsilon^{\frac{1}{2}} - 4k_6\epsilon\right)\sqrt{\bar{V}_o(\bar{x}^o)} \\
&\quad -\frac{\epsilon K_2}{4}\sqrt{\bar{V}_c(e_\xi^c)} - \frac{\epsilon^{\frac{3}{2}} K_2^3}{4}\sqrt{\bar{V}_o(\bar{x}^o)} + k_4\epsilon^{\frac{3}{2}} K_2^4 \int_{t-\tau_M}^{t} \sqrt{\bar{V}_o(\bar{x}^o(s))} ds \\
&\quad +k_3\epsilon K_2 \sum_{i=1}^{N} \chi\|e_{\eta_i}\| \left[\sqrt{V_c(e_\xi)} + \sqrt{V_o(\bar{x}^o)}\right] + \bar{k}_2\epsilon K_2\delta_0 + k_7\epsilon^{\frac{3}{2}} K_2\delta_0
\end{aligned}$$

with $k_3 = \bar{k}_3\sqrt{N}\sqrt{N+1}$.

Selecting $\epsilon < \epsilon^*$ where $\epsilon^* = \min\left\{1, \frac{1}{(4k_4)^2}, \frac{1}{(8k_1)^2}, \frac{1}{8k_5}\right\}$, one can achieve

$$\begin{aligned}
&\frac{d}{dt}\left(\sqrt{\bar{V}_c(e_\xi^c)} + \epsilon^{\frac{3}{2}} K_2^2 \sqrt{\bar{V}_o(\bar{x}^o)}\right) \\
&\leq -\frac{\epsilon K_2}{4}\sqrt{\bar{V}_c(e_\xi^c)} - \frac{\epsilon^{\frac{3}{2}} K_2^3}{4}\sqrt{\bar{V}_o(\bar{x}^o)} + k_4\epsilon^{\frac{3}{2}} K_2^4 \int_{t-\tau_M}^{t} \sqrt{\bar{V}_o(\bar{x}^o(s))} ds \\
&\quad +k_3\epsilon K_2 \sum_{i=1}^{N} \chi\|e_{\eta_i}\| \left[\sqrt{V_c(e_\xi)} + \sqrt{V_o(\bar{x}^o)}\right] + k_2\epsilon K_2\delta
\end{aligned} \tag{44}$$

with $k_2 = \max\{\bar{k}_2, k_7\}$. From Lemma 1, one knows that the attitude error $e_{\eta_i} \to 0$ in finite time which implies that after some time $t > t_a \geq 0$, $\chi\|e_{\eta_i}\| = 0$.

Applying Lemma 2 on (44) with $a = \frac{\epsilon K_2}{4}$, $b = \frac{\epsilon^{\frac{3}{2}} K_2^3}{4}$, $c = k_4\epsilon^{\frac{3}{2}} K_2^4$, $g(t) = k_3\epsilon K_2 \sum_{i=1}^{N} \chi\|e_{\eta_i}\|$ and $k = k_2\epsilon K_2\delta$, one has $\bar{\alpha} > 0$, $\varrho > 0$ and $\gamma \geq 1$ such that for

$$\tau_M < \frac{\bar{\varrho}}{K_2}$$

with $\bar{\varrho} = \frac{\varrho}{4k_4}$, the following inequality is achieved

$$\sqrt{\bar{V}_c(e_\xi^c)} + \epsilon^{\frac{3}{2}} K_2^2 \sqrt{\bar{V}_o(\bar{x}^o)} \leq \bar{\alpha} e^{-\frac{K_1}{8}t} + 8\gamma k_2\delta_0$$

Over-evaluation of the above inequality gives

$$\sqrt{\bar{V}_c(e_\xi^c)} \leq \bar{\alpha} e^{-\frac{K_1}{8}t} + 8\gamma k_2 \delta_0$$
$$K_1 k_8 \sum_{i=1}^{N} \|e_\xi^c\| \leq \bar{\alpha} e^{-\frac{K_1}{8}t} + 8\gamma k_2 \delta_0$$

with $k_8 = \frac{\sqrt{\lambda_{\min} Q}\sqrt{\omega_{\min}}}{\sqrt{N}}$. Hence

$$\sum_{i=1}^{N} \|e_{\xi_i}\| \leq \alpha e^{-\frac{K_1}{8}t} + \frac{\beta \delta_0}{K_1} \tag{45}$$

where $\alpha = \frac{\bar{\alpha}}{K_1 k_8}$ and $\beta = \frac{8k_2\gamma}{k_8}$.

Remark 3 The structure of the proposed observer-based formation tracking controller has some advantages in the presence of communication delays and packet loss during communications. Since, for each agent, the corresponding controller only uses the estimated states provided by the continuous-discrete observers, the time-varying formation tracking is achieved even in the presence of communication delays if measured position data is accurately time stamped. Indeed, in this case, the estimation can be provided as soon as the data is received. Similarly, in case of packet loss, the observer still provides the estimation if the next packet is received before the maximum sample time τ_M.

Remark 4 Inequality (45) shows that the formation tracking error decays exponentially and enters in a ball centered at the origin and will remain there for all future time. This means that practical formation tracking is achieved. One can observe that the radius of the ball is directly proportional to the upper bound of the reference/leader acceleration, i.e. δ_0. This implies that if the leader has a constant velocity then the multi-quadrotor system will achieve exponential stability. The final error can also be reduced by increasing the position controller gain K_1. However, K_1 should always remain less than the observer gain K_2 to keep the controller dynamics slower than the observer dynamics.

5 Simulation results

Let us consider a multi-quadrotor system with three followers denoted from 1 to 3 and a leader denoted as 0. The communication topology among them is shown in Figure 4. It is considered that all the quadrotors in the system have the same structure and modelling parameters. The mass of each quadrotor considered is $m_i = 0.4$ while the inertia matrix is $I_i = diag\{0.0025, 0.0026, 0.0028\}$. The sampling rate at which the position information is transmitted among the

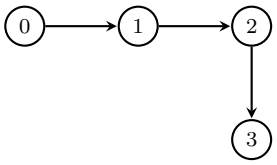


Fig. 4: Communication topology

quadrotors is between $10ms$ and $100ms$. The tuning gains for position controller are chosen as $K_1 = 0.6$, $K_2 = 10$ and $\bar{c} = 1$. The tuning parameters of the attitude controller are selected as $\alpha_3 = \frac{3}{4}$, $\alpha_4 = \frac{6}{7}$, $K_3 = 20$ and $K_4 = 10$.

The desired time-varying formation vector is selected for $i = 1, \ldots, 3$ as given in (10). In the first scenario, the leader is hovering at the altitude of 10m while the followers start from their initial position and make the required formation. Figure 5 shows the formation tracking results while the tracking error is shown in Figure 6.

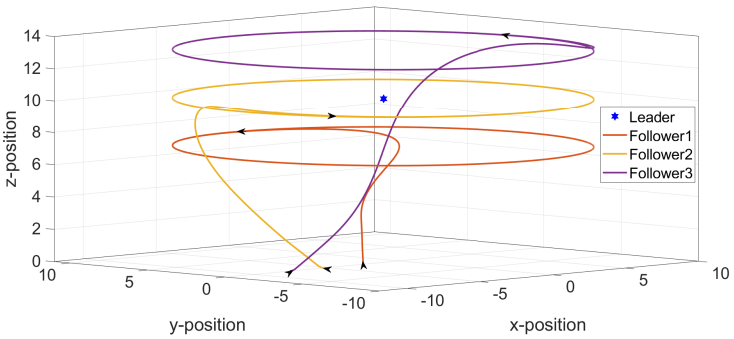


Fig. 5: Formation tracking with a hovering leader

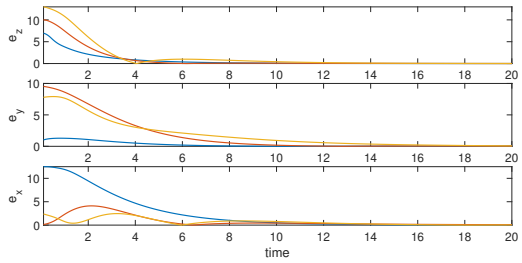


Fig. 6: Tracking error with a stationary leader

In the second scenario, the leader is moving with $\mu_{x0} = 0.03\text{m/s}^2$, $\mu_{y0} = -0.01\text{m/s}^2$, and $\mu_{z0} = 0.03cos(2\pi t/200)\text{m/s}^2$. Figure 7 depicts the formation tracking result. Since the leader is moving with some acceleration, only practical formation tracking is achieved as discussed in Remark 4 and it is evident from the tracking error shown in Figure 8. An example of sampling periods at which the translation position is shared among the quadrotors is illustrated in Figure 9.

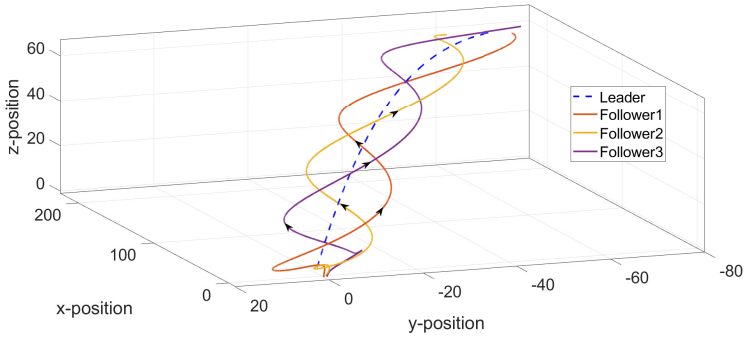


Fig. 7: Formation tracking with a moving leader

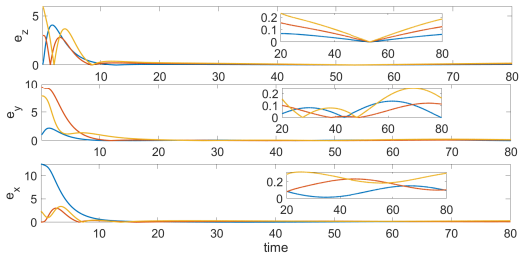
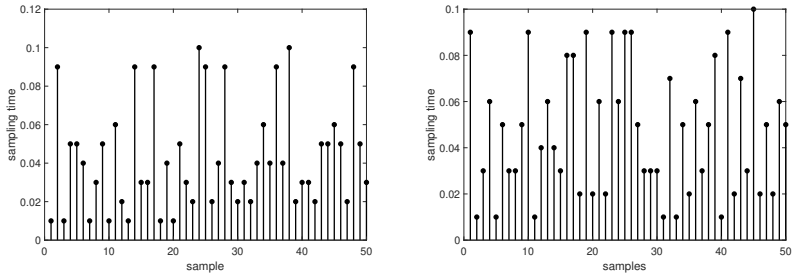


Fig. 8: Tracking error with a moving leader

6 Conclusion

In this paper, a time-varying formation tracking controller for multi-quadrotor systems is discussed. The quadrotors can only send their translation position information to their neighbors at asynchronous and nonuniform sampling rate. The overall control of quadrotor is divided into a position and an attitude control loops. An observer-based position controller is used to achieve the desired formation, while a finite-time controller is used to control the Euler angles



(a) $t_k^{2,1}$ (b) $t_k^{3,2}$

Fig. 9: Sampling periods

of the quadrotor such that it follows the required translation trajectory. A closed-loop stability analysis which includes both position and attitude controllers and the nonlinear coupling strength is provided. Simulation results show the efficiency of the proposed algorithm. The case of switching topology with adaptive gains is planned in the future.

7 Declaration

7.1 Funding

This work was financially supported by European Commission through ECSEL-JU 2018 program under grant agreement No. 826610. The third author was partially supported by the Hauts-de-France region under project ANR I2RM.

7.2 Conflicts of interest

Authors declare that they have no conflict of interest.

7.3 Code availability

Not applicable.

7.4 Authors' Contributions

7.5 Availability of data and material

Not applicable.

7.6 Ethics approval

Not applicable.

7.7 Consent to participate

Not applicable.

7.8 Consent for publication

Not applicable.

Appendix A

Proof Let $v = \min\left(\frac{a}{\sqrt{2}}, \frac{b}{\sqrt{2}}\right), \xi = 2\frac{c\delta}{b}$ and $\kappa = 1-\xi$. Since $\delta \in \left(0, \varrho \min\left(\frac{b}{c}, \frac{1}{\sigma}\right)\right)$, one has

$$0 < 2\frac{c\delta}{b} < 2\frac{c}{b}\varrho \min\left(\frac{b}{c}, \frac{1}{\sigma}\right) \leq 2\varrho \quad \Rightarrow \quad 1 - 2\varrho < \underbrace{1-\xi}_{=\kappa} < 1 \tag{46}$$

$$0 < v\kappa\delta < v\delta < v\varrho \min\left(\frac{b}{c}, \frac{1}{\sigma}\right) \leq \sqrt{2}\varrho \tag{47}$$

Then $\varrho > 0$ can be chosen, independently of a, b, c, k such that for all $\delta \in \left(0, \varrho \min\left(\frac{b}{c}, \frac{1}{\sigma}\right)\right)$ we have

$$\kappa \in \left(\frac{1}{\sqrt{2}}, 1\right) \tag{48}$$

$$e^{v\kappa\delta} \leq 1 + 2v\kappa\delta \tag{49}$$

Consider the following Lyapunov function

$$W(v_t) = v_1^2(t) + v_2^2(t) + c\int_0^\delta \int_{t-s}^t e^{v\kappa(\mu-t+s)} v_2^2(\mu) d\mu ds \tag{50}$$

where $v_t(s) = [v_1(t+s), v_2(t+s)]^T$, $s \in [-\delta, 0]$. One has

$$\dot{W}(v_t) = \frac{d}{dt}\left(v_1^2(t) + v_2^2(t)\right) + c\int_0^\delta \frac{d}{dt}\int_{t-s}^t e^{v\kappa(\mu-t+s)} v_2^2(\mu) d\mu ds.$$

Applying Leibniz integration leads to

$$\begin{aligned}
\dot{W}(v_t) =& -av_1^2(t) - bv_2^2(t) + g(t)(v_1^2(t) + v_2^2(t)) - v\kappa c \int_0^\delta \int_{t-s}^t e^{v\kappa(\mu-t+s)} v_2^2(\mu) d\mu ds \\
&+ c\int_0^\delta e^{v\kappa s} v_2^2(t) - v_2^2(t-s) ds \\
&\leq -av_1^2(t) - bv_2^2(t) + c\int_{t-\delta}^t v_2^2(s) ds + g(t)(v_1^2(t) + v_2^2(t)) + k \\
&\quad - v\kappa c \int_0^\delta \int_{t-s}^t e^{v\kappa(\mu-t+s)} v_2^2(\mu) d\mu ds + c\int_0^\delta e^{v\kappa s} v_2^2(t) ds - c\int_0^\delta v_2^2(t-s) ds \\
\leq& -av_1^2(t) - bv_2^2(t) + g(t) W(v_t) + k + c\left(\frac{e^{v\kappa\delta} - 1}{v\kappa}\right) v_2^2(t) \\
&- v\kappa \left(W(v_t) - v_1^2(t) - v_2^2(t)\right)
\end{aligned}$$

Since $\frac{e^{v\kappa\delta}-1}{v\kappa} \leq 2\delta$ and given the definition of v, the following inequalities are achieved

$$\begin{aligned}
\dot{W}(v_t) + (v\kappa - g(t))\, W(v_t) &\leq (-a + v\kappa)\, v_1^2(t) + (-b + 2c\delta + v\kappa) v_2^2(t) + k \\
\dot{W}(v_t) + (v\kappa - g(t))\, W(v_t) &\leq -a\left(1 - \frac{1}{\sqrt{2}}\right) v_1^2(t) - b\left(1 - (1-\kappa) - \frac{\kappa}{\sqrt{2}}\right) v_2^2(t) + k \\
\dot{W}(v_t) + (v\kappa - g(t))\, W(v_t) &\leq -a\left(\frac{\sqrt{2}-1}{\sqrt{2}}\right) v_1^2(t) - b\kappa\left(\frac{\sqrt{2}-1}{\sqrt{2}}\right) v_2^2(t) + k \\
\dot{W}(v_t) &\leq (-v\kappa + g(t))\, W(v_t) + k
\end{aligned}$$

since $v\kappa \geq \sigma$, so

$$\dot{W}(v_t) \leq (-\sigma + g(t))\, W(v_t) + k$$

To get over-estimation of $W(t)$, let us consider the following differential equation

$$\dot{W}(v_t) + (\sigma - g(t))\, W(v_t) = k$$

The solution of the above differential equation can be given as

$$\begin{aligned}
W(v_t) &= e^{\int_0^t -\sigma + g(\mu) d\mu} W(0) + e^{\int_0^t \sigma + g(\mu) d\mu} \int_0^t e^{\int_0^s \sigma - g(\mu) d\mu} k ds \\
&= e^{\int_0^t -\sigma + g(\mu) d\mu} W(0) + \int_0^t e^{\int_s^t -\bar{\sigma} + g(\mu) d\mu} k ds \qquad (51)
\end{aligned}$$

Furthermore, one has

$$\int_0^t e^{\int_s^t -\sigma+g(\mu)d\mu}kds = \int_0^t e^{-\sigma(t-s)}e^{\int_s^t g(\mu)d\mu}kds$$

and since $g(t) = 0$ for $t > t^*$,

$$\begin{aligned}\int_0^t e^{\int_s^t -\sigma+g(\mu)d\mu}kds &= \int_0^{t^*} e^{-\sigma(t-s)}e^{\int_s^{t^*} g(\mu)d\mu}kds + \int_{t^*}^t e^{-\sigma(t-s)}kds \\ &\leq \bar{\gamma}\int_0^{t^*} e^{-\sigma(t-s)}kds + \int_{t^*}^t e^{-\sigma(t-s)}kds\end{aligned}$$

where $\bar{\gamma} = e^{\int_0^{t^*} g(\mu)d\mu}$. Hence, we have

$$\begin{aligned}\int_0^t e^{\int_s^t -\sigma+g(\mu)d\mu}kds &\leq \bar{\gamma}e^{-\sigma t}\left[\frac{e^{\sigma t^*}}{\sigma}k - \frac{k}{\sigma}\right] + e^{-\sigma t}\left[\frac{e^{\sigma t}}{\bar{\sigma}}k - \frac{e^{\sigma t^*}}{\sigma}k\right] \\ &\leq \frac{\bar{\gamma}k}{\sigma}\left[e^{\sigma(t^*-t)} - e^{-\sigma t}\right] + \frac{k}{\sigma}\left[1 - e^{\sigma(t^*-t)}\right] \qquad (52)\end{aligned}$$

Using (52), (51) becomes

$$\begin{aligned}W(v_t) &\leq \bar{\gamma}e^{-\sigma t}W(0) + \frac{\bar{\gamma}k}{\bar{\sigma}}\left[e^{\sigma(t^*-t)} - e^{-\bar{\sigma}t}\right] + \frac{k}{\bar{\sigma}}\left[1 - e^{\sigma(t^*-t)}\right] \\ &\leq \gamma e^{-\sigma t}W(0) + \frac{\bar{\gamma}k}{\sigma}\left[1 - e^{-\sigma t}\right] \\ &\leq \left(\bar{\gamma}W(0) - \frac{\gamma k}{\sigma}\right)e^{-\sigma t} + \frac{\gamma k}{\sigma} \qquad (53)\end{aligned}$$

where $\gamma = \max\{1, \bar{\gamma}\}$. Choosing $\bar{\alpha} = \bar{\gamma}W(0) - \frac{\gamma k}{\sigma}$ finishes the proof.

Appendix B

One has

$$\begin{aligned}&2K_1(e_\xi)^T[\Omega \otimes QB]F_\Delta \\ &= 2K_1(e_\xi)^T[\Omega \otimes Q][I_N \otimes B]F_\Delta \\ &\leq 2K_1\sqrt{(e_\xi)^T[\Omega \otimes Q]e_\xi}\sqrt{[(I_N \otimes B]F_\Delta]^T[\Omega \otimes Q](I_N \otimes B]F_\Delta}\end{aligned}$$

Using the Cauchy-Schwarz inequality one obtains

$$K_1(e_\xi)^T[(\Omega \otimes (QB)]F_\Delta \leq 2K_1\sqrt{V_c}\sqrt{\lambda_{\max}(\Omega \otimes Q)}\|I_N \otimes B\|\|F_\Delta\|$$

and using Rayleigh inequality one has

$$K_1(e_\xi)^T[(\Omega \otimes (QB)]F_\Delta \leq 2K_1\sqrt{V_c}\sqrt{\omega_{\max}\lambda_{\max}(Q)}\|F_\Delta\| \qquad (54)$$

Over estimation of term $\|F_\Delta\|$ gives

$$\|F_\Delta\| \leq \sum_{i=1}^{N} \left\| \frac{T_i}{m_i} H_i \right\|$$

with

$$\left\| \frac{T_i}{m_i} H_i \right\| = \frac{1}{m_i} |T_i(e_{\xi_i})| \|H_i\| \tag{55}$$

$$= \frac{1}{m_i} |T_i(e_{\xi_i})| \sqrt{h_1^2 + h_2^2 + h_3^2} \tag{56}$$

where

$$|T_i(e_{\xi_i})| = m_i \|\mu_i + g e_3\| = m_i \sqrt{\mu_{x_i}^2 + \mu_{y_i}^2 + (\mu_{z_i} + g)^2}. \tag{57}$$

Following the proof of [26, Theorem 1], one has

$$\|\mu_i\| = \|\mu_i^f\| \leq c_4 \sum_{i=1}^{N} \|e_{\xi_i}\| + c_5 \sum_{k=0}^{N} s_{i,k} \|\bar{x}_{i,k}\| \tag{58}$$

where $c_4, c_5 > 0$. So, we obtain

$$\|T_i\| \leq m_i \left(g + c_6 \left\{ \sum_{i=1}^{N} \|e_{\xi_i}\| + \sum_{k=0}^{N} s_{i,k} \|\bar{x}_{i,k}\| \right\} \right) \tag{59}$$

$$\leq l_1 \left(r_1 + \sum_{i=1}^{N} \|e_{\xi_i}\| + \sum_{k=0}^{N} s_{i,k} \|\bar{x}_{i,k}\| \right) \tag{60}$$

where $c_6 = max(c_4, c_5)$, $l_1 = m_i c_6$ and $r_1 = m_i g / l_1$. From these inequalities, one can deduce that

$$|T_i(e_{\xi_i})| \leq \begin{cases} r_2 \bar{e}_i \text{ for } \bar{e}_i \geq r_1 \\ r_1 r_2 \text{ for } \bar{e}_i < r_1 \end{cases} \tag{61}$$

where $\bar{e}_i = \sum_{i=1}^{N} \|e_{\xi_i}\| + \sum_{k=0}^{N} \|\bar{x}_{i,k}\|$ and $r_2 = 2 l_1$.

Now replacing $(\phi_i, \theta_i, \psi_i)$ with $(\phi_{di} + e_{\phi_i}, \theta_{di} + e_{\theta_i}, \psi_{di} + e_{\psi_i})$ and using the following trigonometric equalities

$$sin(a+b) = sin(a) + sin\left(\frac{b}{2}\right) cos\left(a + \frac{b}{2}\right) \tag{62}$$

$$cos(a+b) = cos(a) - sin\left(\frac{b}{2}\right) sin\left(a + \frac{b}{2}\right) \tag{63}$$

then h_3 can be written as

$$\begin{aligned} h_3 &= c\phi_i c\theta_i - c\phi_{di} c\theta_{di} \\ &= c(\phi_{di} + e_{\phi_i}) c(\theta_{di} + e_{\theta_i}) - c\phi_{di} c\theta_{di} \\ &= [c\phi_{di} - s(e_{\phi_i}/2) s(\phi_{di} + e_{\phi_i}/2)][c\theta_{di} - s(e_{\theta_i}/2) s(\theta_{di} + e_{\theta_i}/2)] - c\phi_{di} c\theta_{di} \\ &= -c\phi_{di} s(e_{\theta_i}/2) s(\theta_{di} + e_{\theta_i}/2) - c\theta_{di} s(e_{\phi_i}/2) s(\phi_{di} + e_{\phi_i}/2) \\ &\quad + [-s(e_{\phi_i}/2) s(\phi_{di} + e_{\phi_i}/2)][s(e_{\theta_i}/2) s(\theta_{di} + e_{\theta_i}/2)] \end{aligned}$$

Using the following trivial inequalities

$$|\sin(a)| \leq |a|, \qquad |\sin(a)| \leq 1, \qquad |\cos(a)| \leq 1$$
$$|a||b| \leq \frac{1}{2}(|a| + |b|) \text{ for } |a| \leq 1, |b| \leq 1$$
$$|a||b||c| \leq \frac{1}{2}(|a| + |b| + |c|) \text{ for } |a| \leq 1, |b| \leq 1, |c| \leq 1 \tag{64}$$

one gets

$$\begin{aligned} |h_3| &\leq |s(e_{\phi_i}/2)| + |s(e_{\theta_i}/2)| + |s(e_{\phi_i}/2)||s(e_{\theta_i}/2)| \\ &\leq |s(e_{\phi_i}/2)| + |s(e_{\theta_i}/2)| + \frac{1}{2}(|s(e_{\phi_i}/2)| + |s(e_{\theta_i}/2)|) \\ &\leq \frac{3}{2}(|s(e_{\phi_i}/2)| + |s(e_{\theta_i}/2)|) \\ &\leq \frac{3}{4}(|e_{\phi_i}| + |e_{\theta_i}|) \end{aligned} \tag{65}$$

Therefore, the following inequality can be obtained

$$\begin{aligned} h_3^2 &\leq \frac{9}{16}(e_{\phi_i}^2 + e_{\theta_i}^2 + 2|e_{\phi_i}||e_{\theta_i}|) \\ &\leq \frac{9}{8}(e_{\phi_i}^2 + e_{\theta_i}^2) \\ &\leq \varsigma_3(e_{\phi_i}^2 + e_{\theta_i}^2 + e_{\psi_i}^2) \end{aligned} \tag{66}$$

where $\varsigma_3 = \frac{9}{8}$. Similarly, one can show that

$$h_2^2 \leq \varsigma_2(e_{\phi_i}^2 + e_{\theta_i}^2 + e_{\psi_i}^2) \tag{67}$$
$$h_1^2 \leq \varsigma_1(e_{\phi_i}^2 + e_{\theta_i}^2 + e_{\psi_i}^2) \tag{68}$$

Therefore, one gets

$$\begin{aligned} \|H(e_{\xi_i}, e_{\eta_i})\| &= \sqrt{h_1^2 + h_2^2 + h_3^2} \\ &\leq \sqrt{\varsigma_1(e_{\phi_i}^2 + e_{\theta_i}^2 + e_{\psi_i}^2) + \varsigma_2(e_{\phi_i}^2 + e_{\theta_i}^2 + e_{\psi_i}^2) + \varsigma_3(e_{\phi_i}^2 + e_{\theta_i}^2 + e_{\psi_i}^2)} \\ &\leq c_7\|\eta_i - \eta_{d_i}\| \end{aligned} \tag{69}$$

with $c_7 = \sqrt{\varsigma_1 + \varsigma_2 + \varsigma_3}$

From (61) and (69), one can show that for $\bar{e}_i \geq r_1$

$$\begin{aligned} \left\| \frac{T_i}{m_i} H_i \right\| &\leq \frac{1}{m_i} r_2 \bar{e}_i c_7 \|e_{\eta_i}\| \\ &\leq c_8 \|e_{\eta_i}\| \bar{e}_i \end{aligned}$$

with $c_8 = \frac{1}{m_i} r_2 c_7$. So one has

$$\left\| \frac{T_i}{m_i} H_i \right\| \leq c_8 \|e_{\eta_i}\| \left[\sum_{i=1}^{N} \|e_{\xi_i}\| + \sum_{k=0}^{N} s_{i,k} \|\bar{x}_{i,k}\| \right] \tag{70}$$

Since

$$\sum_{i=1}^{N} \|e_{\xi_i}\| \leq \frac{\sqrt{N}}{\sqrt{\lambda_{\min}(Q)}\sqrt{\omega_{\min}}} \sqrt{V_c(e_\xi^c)}$$

and

$$\|\bar{x}_{i,k}\| \leq \frac{1}{\sqrt{\lambda_{\min}(P)}} \sqrt{V_o(\bar{x}_{i,k})}$$

inequality (70) becomes

$$\left\| \frac{T_i}{m_i} H_i \right\| \leq c_8 c_9 \|e_{\eta_i}\| \left[\sqrt{V_c(e_\xi^c)} + \sum_{k=0}^{N} s_{i,k} \sqrt{V_o(\bar{x}_{i,k})} \right]$$

with $c_9 = \max\left(\frac{\sqrt{N}}{\sqrt{\lambda_{\min}(Q)}\sqrt{\omega_{\min}}}, \frac{1}{\sqrt{\lambda_{\min}(P)}} \right)$. On can write the above inequality as

$$\left\| \frac{T_i}{m_i} H_i \right\| \leq \chi \|e_{\eta_i}\| \left[\sqrt{V_c(e_\xi^c)} + \sum_{k=0}^{N} s_{i,k} \sqrt{V_o(\bar{x}_{i,k})} \right] \tag{71}$$

where $\chi = c_8 c_9$ which leads to

$$\|F_\Delta\| \leq \sum_{i=1}^{N} \chi(\|e_{\eta_i}\|) \left[\sqrt{V_c(e_\xi^c)} + \sum_{k=0}^{N} s_{i,k} \sqrt{V_o(\bar{x}_{i,k})} \right] \tag{72}$$

Hence, inequality (54) is achieved.

References

1. Zhao, Z., Cao, D., Yang, J., Wang, H.: High-order sliding mode observer-based trajectory tracking control for a quadrotor uav with uncertain dynamics. Nonlinear Dynamics **102**(4), 2583–2596 (2020)
2. Shakhatreh, H., Sawalmeh, A.H., Al-Fuqaha, A., Dou, Z., Almaita, E., Khalil, I., Othman, N.S., Khreishah, A., Guizani, M.: Unmanned aerial vehicles (uavs): A survey on civil applications and key research challenges. Ieee Access **7**, 48572–48634 (2019)
3. Mishra, B., Garg, D., Narang, P., Mishra, V.: Drone-surveillance for search and rescue in natural disaster. Computer Communications **156**, 1–10 (2020)
4. Eskandarpour, A., Sharf, I.: A constrained error-based mpc for path following of quadrotor with stability analysis. Nonlinear Dynamics **99**(2), 899–918 (2020)
5. Iskandarani, M., Hafez, A.T., Givigi, S.N., Beaulieu, A., Rabbath, C.A.: Using multiple quadrotor aircraft and linear model predictive control for the encirclement of a target. In: 2013 IEEE International Systems Conference (SysCon), pp. 620–627. IEEE (2013)

6. Hou, Z., Wang, W., Zhang, G., Han, C.: A survey on the formation control of multiple quadrotors. In: 2017 14th International Conference on Ubiquitous Robots and Ambient Intelligence (URAI), pp. 219–225. IEEE (2017)
7. Sivakumar, A., Tan, C.K.Y.: Uav swarm coordination using cooperative control for establishing a wireless communications backbone. In: Proceedings of the 9th International Conference on Autonomous Agents and Multiagent Systems: Volume 3-Volume 3, pp. 1157–1164 (2010)
8. Yao, X.Y., Ding, H.F., Ge, M.F.: Fully distributed control for task-space formation tracking of nonlinear heterogeneous robotic systems. Nonlinear Dynamics **96**(1), 87–105 (2019)
9. Lippay, Z.S., Hoagg, J.B.: Leader-following formation control with time-varying formations and bounded controls for agents with double-integrator dynamics. In: 2020 American Control Conference (ACC), pp. 871–876. IEEE (2020)
10. Van Vu, D., Trinh, M.H., Nguyen, P.D., Ahn, H.S.: Distance-based formation control with bounded disturbances. IEEE Control Systems Letters **5**(2), 451–456 (2020)
11. Li, S., Zhang, J., Li, X., Wang, F., Luo, X., Guan, X.: Formation control of heterogeneous discrete-time nonlinear multi-agent systems with uncertainties. IEEE Transactions on Industrial Electronics **64**(6), 4730–4740 (2017)
12. Yu, J., Dong, X., Li, Q., Ren, Z.: Practical time-varying formation tracking for high-order nonlinear multi-agent systems based on the distributed extended state observer. International Journal of Control **92**(10), 2451–2462 (2019)
13. Qin, D., Liu, A., Zhang, D., Ni, H.: Formation control of mobile robot systems incorporating primal-dual neural network and distributed predictive approach. Journal of the Franklin Institute **357**(17), 12454–12472 (2020)
14. Nag, S., Summerer, L.: Behaviour based, autonomous and distributed scatter manoeuvres for satellite swarms. Acta Astronautica **82**(1), 95–109 (2013)
15. Mercado, D., Castro, R., Lozano, R.: Quadrotors flight formation control using a leader-follower approach. In: 2013 European Control Conference (ECC), pp. 3858–3863. IEEE (2013)
16. Ren, W.: Consensus strategies for cooperative control of vehicle formations. IET Control Theory & Applications **1**(2), 505–512 (2007)
17. Du, H., Li, S., Lin, X.: Finite-time formation control of multiagent systems via dynamic output feedback. International Journal of Robust and Nonlinear Control **23**(14), 1609–1628 (2013)
18. Dong, X., Zhou, Y., Ren, Z., Zhong, Y.: Time-varying formation tracking for second-order multi-agent systems subjected to switching topologies with application to quadrotor formation flying. IEEE Transactions on Industrial Electronics **64**(6), 5014–5024 (2016)
19. Xiong, T., Pu, Z., Yi, J., Tao, X.: Fixed-time observer based adaptive neural network time-varying formation tracking control for multi-agent

systems via minimal learning parameter approach. IET Control Theory & Applications **14**(9), 1147–1157 (2020)
20. Lai, J., Chen, S., Lu, X., Zhou, H.: Formation tracking for nonlinear multi-agent systems with delays and noise disturbance. Asian Journal of Control **17**(3), 879–891 (2015)
21. Kuriki, Y., Namerikawa, T.: Consensus-based cooperative formation control with collision avoidance for a multi-uav system. In: 2014 American Control Conference, pp. 2077–2082. IEEE (2014)
22. Wang, Y., Wu, Q., Wang, Y.: Distributed cooperative control for multiple quadrotor systems via dynamic surface control. Nonlinear Dynamics **75**(3), 513–527 (2014)
23. Zou, Y., Zhou, Z., Dong, X., Meng, Z.: Distributed formation control for multiple vertical takeoff and landing uavs with switching topologies. IEEE/ASME Transactions on Mechatronics **23**(4), 1750–1761 (2018)
24. Zhang, W., Chaoyang, D., Maopeng, R., Yang, L.: Fully distributed time-varying formation tracking control for multiple quadrotor vehicles via finite-time convergent extended state observer. Chinese Journal of Aeronautics **33**(11), 2907–2920 (2020)
25. Cong, Y., Du, H., Jin, Q., Zhu, W., Lin, X.: Formation control for multiquadrotor aircraft: Connectivity preserving and collision avoidance. International Journal of Robust and Nonlinear Control **30**(6), 2352–2366 (2020)
26. Ajwad, S.A., Menard, T., Moulay, E., Defoort, M., Coirault, P.: Observer based leader-following consensus of second-order multi-agent systems with nonuniform sampled position data. Journal of the Franklin Institute **356**(16), 10031–10057 (2019)
27. Ajwad, S.A., Moulay, E., Defoort, M., Ménard, T., Coirault, P.: Output-feedback formation tracking of second-order multi-agent systems with asynchronous variable sampled data. In: 2019 IEEE 58th Conference on Decision and Control (CDC), pp. 4483–4488. IEEE (2019)
28. Ajwad, S.A., Moulay, E., Defoort, M., Ménard, T., Coirault, P.: Collision-free formation tracking of multi-agent systems under communication constraints. IEEE Control Systems Letters **5**(4), 1345–1350 (2020)
29. Menard, T., Ajwad, S.A., Moulay, E., Coirault, P., Defoort, M.: Leader-following consensus for multi-agent systems with nonlinear dynamics subject to additive bounded disturbances and asynchronously sampled outputs. Automatica **121**, 109176 (2020)
30. Kendoul, F.: Nonlinear hierarchical flight controller for unmanned rotorcraft: design, stability, and experiments. Journal of guidance, control, and dynamics **32**(6), 1954–1958 (2009)
31. Zhao, B., Xian, B., Zhang, Y., Zhang, X.: Nonlinear robust adaptive tracking control of a quadrotor uav via immersion and invariance methodology. IEEE Transactions on Industrial Electronics **62**(5), 2891–2902 (2014)
32. Ren, W., Beard, R.W.: Distributed consensus in multi-vehicle cooperative control, vol. 27. Springer (2008)

33. Song, Q., Liu, F., Cao, J., Yu, W.: Pinning-controllability analysis of complex networks: an m-matrix approach. IEEE Transactions on Circuits and Systems I: Regular Papers **59**(11), 2692–2701 (2012)
34. Zhang, H., Li, Z., Qu, Z., Lewis, F.L.: On constructing lyapunov functions for multi-agent systems. Automatica **58**, 39–42 (2015)